International Journal of Nanomedicine

Dovepress
open access to scientific and medical research

Open Access Full Text Article

ORIGINAL RESEARCH

A TSHR-Targeting Aptamer in Monocytes Correlating with Clinical Activity in TAO

Jiamin Cao, Feng Zhang, Haiyan Chen, Bingxuan Wu, Jiayang Yin, Changci Chenzhao, Wei Xiong

Department of Ophthalmology, Central South University, Changsha City, People's Republic of China

Correspondence: Wei Xiong, Email weixiong420@csu.edu.cn

Background: Manifestations of thyroid-associated ophthalmopathy (TAO) vary greatly. Few tools and indicators are available to assess TAO, restricting personalized diagnosis and treatment.

Aim: To identify an aptamer targeting thyroid-stimulating hormone receptor (TSHR) and utilize this aptamer to evaluate clinical activity in patients with TAO.

Methods: An aptamer targeting TSHR was developed by exponential enrichment and systematic evaluation of TSHR ligands. After truncation and optimization, the affinity, equilibrium dissociation constant, and serum stability of this aptamer were evaluated. The affinity of the TSHR-targeting aptamer to isolated fibrocytes was assessed, as was aptamer internalization by fibrocytes. The mechanism of binding was determined by molecular docking. The correlation between disease manifestations and the percentage of TSHR-positive cells was assessed by correlation analysis.

Results: The aptamer TSHR-21-42 was developed to bind to TSHR, with the equilibrium dissociation constant being 71.46 Kd. Isolated fibrocytes were shown to bind TSHR-21-42 through TSHR, with its affinity maintained at various temperatures and ion concentrations. TSHR-21-42 could compete with anti-TSHR antibody, both for binding site to TSHR and uptake by cells after binding. In addition, TSHR-21-42 could bind to leukocytes in peripheral blood, with this binding differing in patients with TAO and healthy control subjects. The percentage of TSHR-positive monocytes, as determined by binding of TSHR-21-42, correlated positively with clinical activity score in patients with TAO, indicating that TSHR-21-42 binding could assess the severity of TAO.

Conclusion: This aptamer targeting TSHR may be used to objectively assess disease activity in patients with TAO, by evaluating the percentages of TSHR positive cells in peripheral blood.

Keywords: thyroid-associated ophthalmopathy, thyroid-stimulating hormone receptor, aptamer, clinical activity score, precision medicine

Introduction

Thyroid-associated ophthalmopathy (TAO) is a type of autoimmune disease affecting various organs.[1] The pathogenesis of TAO has been found to involve adipose tissue in the muscles and orbit, resulting in exophthalmos and diplopia, respectively. Immune system dysfunction, as revealed in both the orbit and circulation, has been associated with the pathogenesis of TAO. For example, programmed cell death 1 ligand 1 (PD1-L1) has been found to inhibit the function of T cells in TAO, and application of the anti-CD20 B cell-depleting monoclonal antibody rituximab has been used to treat TAO.[2,3] Immune system dysfunction was shown to upregulate oxidative stress levels, which damage tissues and cells in the orbit.[4,5] During the process of tissue damage repair, CD34+ fibroblasts derived from fibrocytes in bone marrow could be differentiated into myofibroblasts and adipocytes by treatment with TGF-β and PPAR-γ, respectively, with higher levels of fibrosis and adipogenesis in the orbit being associated with higher degrees of disease manifestations.[6]

Thyroid-stimulating hormone receptor (TSHR) is a type of G-protein coupled receptor, with higher levels of anti-TSHR antibody being associated with autoimmune processes. Because TSHR is present in both the thyroid and orbit, patients with TAO may have thyroid dysfunction. TSHR also interacts with insulin-like growth factor 1 (IGF-1), with the binding of IGF-1 to TSHR being a key step during the onset of TAO. This led to the development of the anti-IGF-1

Received: 9 November 2023
Accepted: 28 February 2024
Published: 17 April 2024

monoclonal antibody teprotumumab, which binds to IGF-1 receptors, for treatment of TAO.[7,8] TSHR on the surface of fibroblasts has been associated with pathological changes, including edema, fibrosis, and adipogenesis, suggesting that drugs targeting TSHR may be important in treating TAO.[9] Increased levels of anti-TSHR antibody have been associated with increased severity of TAO, suggesting that anti-TSHR antibody may serve as a link between the thyroid and orbit.[10–12] TSHR on fibrocytes and fibroblasts has been found to regulate biological processes and cell function, suggesting that TSHR levels may better reflect disease status and that TSHR may be a key to the pathogenesis of TAO. It is unclear, however, disease can be evaluated by measuring levels of TSHR or whether TSHR-specific white blood cells (WBC) could serve as biomarkers of the severity of TAO.

The clinical stages of TAO have been characterized as active and inactive based on their clinical activity scores (CAS), with treatment methods depending on the different stages of TAO. Glucocorticoid compounds are usually the first-line therapy during the active stage of TAO, whereas surgery is usually the treatment of choice during inactive stages of TAO.[13] Thus, correctly identifying the clinical stage is essential for optimal therapy in individual patients. Many manifestations of TAO, however, are relatively non-specific, such as redness of the conjunctiva. Similar CAS scores may mask clinical differences, especially in patients at the junction of active and inactive periods. Thus more objective indicators are needed to evaluate the manifestations and severity of TAO.

Clinical stages of TAO can be evaluated by measuring levels of TSHR. For example, TSHR levels in fibrocytes were found to be higher in patients with than without TAO, with alterations in TSHR levels associated with alterations in the immune system.[14] The percentage of TSHR-positive peripheral blood mononuclear cells (PBMCs) was found to correlate positively with CAS, suggesting that TSHR may be used to evaluate TAO.[15] These studies, however, evaluated TSHR levels using anti-TSHR antibody, which is expensive and uneditable, limiting the clinical use of this reagent. It is therefore necessary to identify optimized substitutes.

An aptamer is a type of single chain DNA or RNA, with advantages that include high affinity to the targeted molecule, low cost, and the ability to be edited.[16] The binding abilities of aptamers are similar to those of antibodies, but aptamers are easier to synthesize and have a smaller batch effect than antibodies, suggesting that aptamers have potential clinical application.[17] In addition, aptamer-related drugs such as neo5 and E10030 have been used clinically or undergoing clinic trials.[18] Additional aptamers have been obtained through processes such as the systematic evolution of ligands by exponential enrichment (SELEX), with aptamers recently utilized in the development of biosensors, drugs, and reagents.[19] For example, the AS1411 functionalized triangle DNA origami was used to develop imaging-guided chemo-phototherapy.[20] The ability to edit aptamers has resulted in a wider range of applications, such as measuring the levels of expression level of fluorophore-labeled proteins.[21] To date, however, aptamers with high affinity towards TSHR have not been developed or utilized. The present study describes the use of SELEX to develop and optimize an aptamer targeting TSHR and to evaluate the ability of this anti-TSHR aptamer to determine the stage of TAO and to develop objective criteria that could be used to determine a precise therapeutic strategy for patients with this condition.

Methods

Selex

The TSHR targeting aptamer was obtained using the SELEX process.[22] TSHR protein (Sangon Biotech, China) was the positive target and human serum albumin (HSA) was the negative target. Proteins were linked to magnetic beads through amide bonds. During each round, the aptamer was denatured at 95°C for 10 min and renatured on ice for 10min. The aptamer was incubated with the negative target (HSA) at room temperature, and the supernatant was collected and incubated with the positive target. Aptamer binding to the positive target was collected following denaturation and renaturation, as above. The resulting aptamer was amplified by PCR, and the resulting product was used during the next round of screening. As the number of screenings increased, the time of incubation was decreased, from 50 min to 30 min. To reduce any nonspecific binding between the aptamer and the target, serum was added during the final rounds of screening. Affinity was determined through surface plasmon resonance (SPR). The library with the highest affinity to TSHR was defined as the screening endpoint library, which was used to sequence and select the aptamer.

Fibrocyte Isolation and Cultivation

Fibrocytes was mainly isolated from PBMC preparations. Briefly, a 3 mL aliquot of human PBMC separation medium (Solarbio, China) was added to each centrifuge tube, followed by the slow addition of an equal volume of peripheral blood and centrifugation at 750 g for 30 min. PBMCs were decanted, washed with PBS and cultivated at 37°C in complete medium (DMEM containing 5% fetal bovine serum and 1% penicillin-streptomycin) in an atmosphere containing 5% CO_2. After 7 days, the medium was replaced by fresh complete medium; after 12–14 days, the attached cells were treated with Accutase (Yeasen, China) and collected by mechanical scraping.

Blood Samples

Patients with TAO were included if they were diagnosed with this condition according to Chinese guidelines[23] and were willing to participate in the study. Patients were excluded if they had experienced major trauma or surgery within 3 months of enrollment; had other systematic immune diseases or cancer; or had received high-dose systemic glucocorticoid therapy during the previous 3 months. Healthy controls were included if they had normal thyroid function; but were excluded if they had thyroid-related disease, a dysfunction of the thyroid, a systematic immune disease or cancer; or had experienced major trauma or surgery within 3 months. A 5 mL aliquot of peripheral blood was collected from TAO patients and healthy controls into an anticoagulant tube (EDTAK2) at Third Xiangya Hospital. The blood samples were stored at 4°C and processed within 24h.

Clinical Information

All patients and healthy controls who participated in the study signed informed consent forms. Clinical information collected from each subject included demographic characteristics (age, sex, race) and disease characteristics (including the duration, CAS, and severity of TAO, duration and dose of glucocorticoid treatment, operation history, and trauma history). CAS was evaluated by one chief physician, with 1 indicating spontaneous retrobulbar pain, 2 indicating pain on attempted upward or downward gaze, 3 indicating redness of eyelids, 4 indicating redness of the conjunctiva, 5 indicating swelling of the caruncle or plica, 6 indicating swelling of the eyelids, and 7 indicating swelling of the conjunctiva (chemosis).[23,24] Patients with CAS <3 points were regarded as being in the inactive phase of TAO, whereas patients with CAS ≥3 points were regarded as being in the active phase of disease. TAO severity was determined using EUGOGO criteria.

Optimization of Sequence

The secondary structure of the aptamer sequence was visualized using RNAfold.[25] The end sequence was removed and the core sequence preserved, resulting in retention of the functional structure, such as the loop structure. The affinity of the optimized aptamer to the target was determined after optimization.

Serum Stability

Aptamer was added to serum at a concentration of 3 μM aptamer, and the serum samples were incubated at 37°C for 0, 2, 4, 6, 8, 10, 12, 24, 48, and 72 h. Aptamer was collected from each sample by agarose gel electrophoresis. The gray value of aptamer calculated using Image J software was regarded as the relative quantity, which was used to evaluate the stability of aptamer in serum.

Determination of Equilibrium Dissociation Constant

Fibrocytes were incubated with 0, 15.6, 31.3, 62.5, 125, or 250 nM aptamer for 30 min at 25°C. After washing with DPBS, the fluorescence intensity of the fibrocytes was measured. The affinity between the aptamer and fibrocytes was determined by calculating the equilibrium dissociation constant using the formula, $Y = \frac{V_{max}X}{K_d+X}$, where Y was the fluorescence intensity determined by flow cytometry, X was the concentration of aptamer, V_{max} was the maximum value of Y, and K_d was the equilibrium dissociation constant.

Immunofluorescence Staining

Adherent fibrocytes were washed twice with PBS, fixed with paraformaldehyde for 30 min, washed and incubated with 0.5% Triton-100 for 10 min. Non-specific binding was blocked by incubation with bovine serum albumin (BSA) for 1 h. The fibrocytes were washed thrice with PBS and incubated with antibodies to CD45, collagen I, TSHR, and CD34 (each from Proteintech, Wuhan, China) for 24 h at 4°C. The fibrocytes were again washed thrice with PBS and incubated with anti-rabbit secondary antibody (Multi Sciences, China) for 1 h at room temperature. Nuclei were subsequently stained with DAPI (Solarbio) for 5 min.

For staining with aptamer, aptamer was denatured at 95°C for 10 min and renatured on ice for 10 min. Fibrocytes were washed with PBS three times and incubated with 250 nM aptamer for 30 min at room temperature. The cells were washed with PBS, and the nuclei were stained with DAPI (Solarbio) for 5 min. Fluorescence was evaluated using a fluorescence microscope.

Flow Cytometry

Peripheral blood was mixed 1:3 with red blood cell lysis buffer (Solar, China) and incubated at room temperature for 10 min. Each mixture was centrifuged for 10 min at 450 g. The precipitate was collected and washed with red blood cell lysis buffer and PBS. The resulting leukocyte preparations were incubated with antibodies to CD45 and CD34 (both from Biolegend, US). Alternatively, the leukocyte preparations were incubated in fixation/permeabilization solution for 20 min, washed with Perm/Wash buffer (BD Biosciences, US), and incubated with anti-collagen I antibody (Millipore, US) for 30 min. The cells were washed twice and incubated with anti-TSHR antibody (Novus Biologicals, US), aptamer, or the aptamer library. After washing with Perm/Wash buffer, the cells were evaluated by flow cytometry.

To test fibrocytes, the aptamer was denatured at 95°C for 10 min, renatured on ice for 10 min, and incubated with suspensions of fibrocytes for 30 min at room temperature. After washing twice with DPBS, the fibrocytes were evaluated by flow cytometry.

Identification of Protein Targeted by the Aptamer

Adherent fibrocytes were washed with DPBS and membrane proteins were obtained by incubation in low permeability buffer (5% 1.5 M Tris-HCl (Solarbio), 1×PMSF (Solarbio) and 1×cocktail (Abcam, England) of DPBS) and lysis buffer (1% Triton-100 (ThermoFisher, US) in low permeability buffer). Biotin-aptamer was coupled to Streptavidin-Sepharose Beads (GE Healthcare, US), followed by denaturation and renaturation. The beads were incubated with membrane proteins for 30 min at 4°C, washed three times with DPBS, denatured at 95°C for 10 min and renatured on ice for 10 min. The beads were centrifuged at 4000 rpm for 3 min, and the supernatants were collected and evaluated by SDS-PAGE. The gels were stained with Coomassie brilliant blue and washed with water for 24 h, and the aptamer-binding proteins were determined.

Molecular Docking

The 3D structure of the aptamer was simulated using Avogadro.[26] The 3D structure of THSR was downloaded from PDB (https://www.rcsb.org/). Molecular docking was performed by extracting the F-chain of TSHR (PDB ID: 7XW6) through chimera 1.16. with the procedure performed using HDOCK (http://hdock.phys.hust.edu.cn/).[27]

Statistical Analyses

Data were reported as mean ± standard deviation or percentage. Differences between groups were determined using *t*-tests. Sample sizes were determined using an online tool (http://powerandsamplesize.com/). Correlations between CAS and positive monocytes were determined by simple linear regression. Sample sizes were determined as described,[28,29] with the number of samples being >10 for simple linear regression. Pearson correlation analysis was performed to determine whether the aptamer had the same capacity as the anti-TSHR antibody. All statistical analyses were performed using GraphPad Prism 9.0 software, with $P<0.05$ defined as statistically significant.

Results

Development of an Anti-TSHR Aptamer with SELEX

TSHR or BSA was linked to agarose beads through amide bonds, with these beads defined as the positive and negative targets, respectively. Six screening rounds of the SELEX process were performed (Figure 1A), increasing the affinity between the DNA library and the positive target, with the maximum value attained at the fifth round through SPR. The dissociation speed was slower during the sixth than during the fifth round of screening, with the library obtained during the sixth round being further evaluated (Figure 1B). Of the total of 319,808 sequences evaluated, high throughput screening identified 2985 types of sequences. A total of 130 types of sequences were synthesized and their affinity to TSHR measured. The first set of 80 aptamers had a low affinity (<30 RU) to THSR (Supplementary Figure 1). Evaluation of the second set of 50 aptamers identified two aptamers, TSHR-18 and TSHR-21, with high affinity (>50 RU) to TSHR (Figure 1C).

Optimization of Aptamers and Identification of Their Characteristics

To optimize aptamers, the sequences of aptamers were truncated based on their secondary structures, as determined using RNAFold (Figure 2A), with the original and truncated sequences presented (Supplementary Table 1). Evaluation of the affinity of the optimized aptamers to TSHR showed that TSHR-21-42 had the highest affinity (Figure 2B), with an equilibrium dissociation constant of TSHR-21-42 with TSHR of 76.48 nM (Figure 2C). Evaluation of its stability in serum showed that the aptamer was gradually degraded. After 2 h in serum, over 10% of the TSHR-21-42 was degraded;

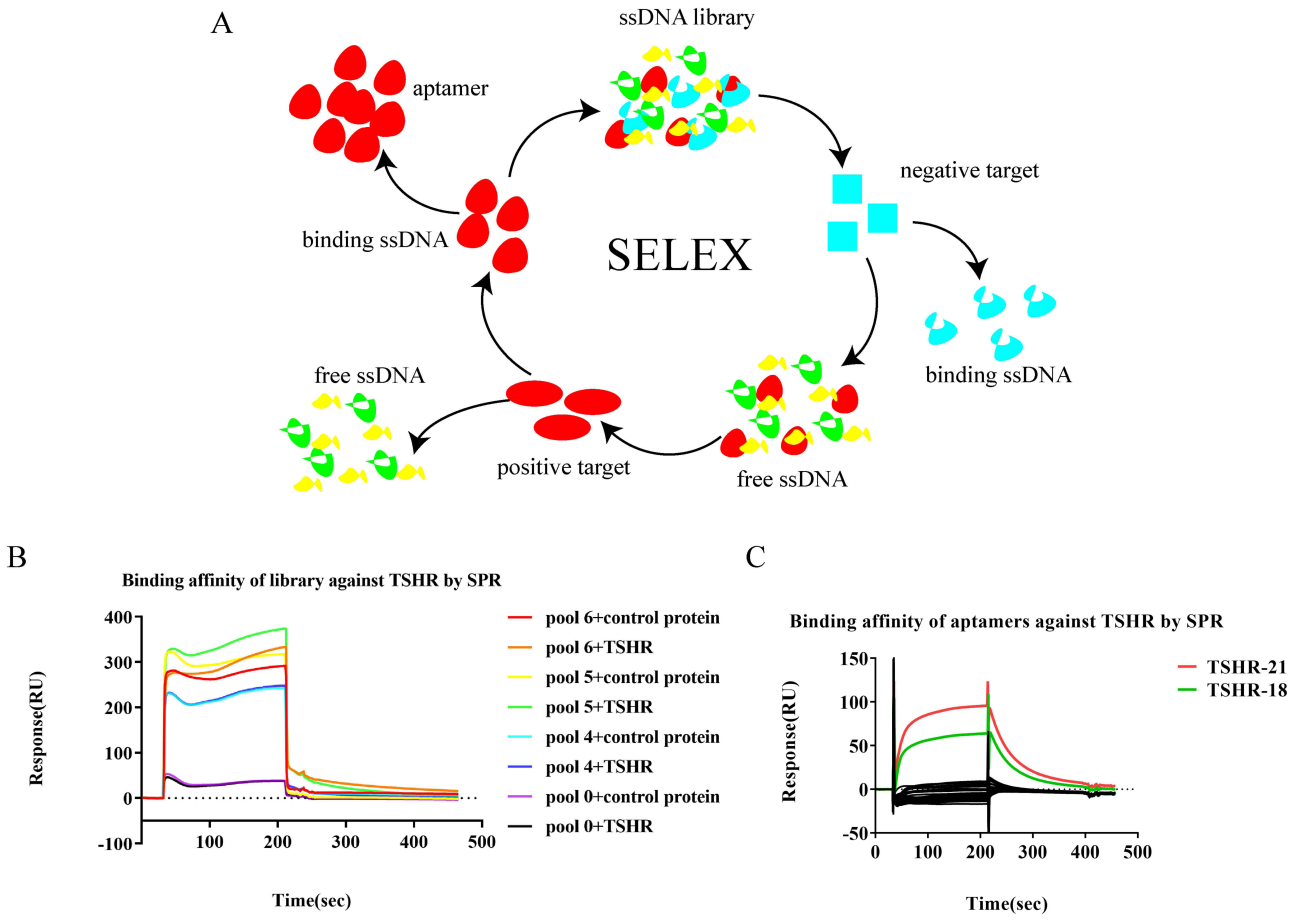

Figure 1 Development of an aptamer through SELEX. (**A**) Single stranded DNA (ssDNA) libraries were incubated with the negative (human serum albumin) and positive (TSHR) targets. Aptamers that bound to the negative target were abandoned and those that bound to the positive target retained. (**B**) Performance of six screening rounds of SELEX, with the affinity of the product to TSHR measured. (**C**) SPR determination of the affinity of 50 aptamers to TSHR.

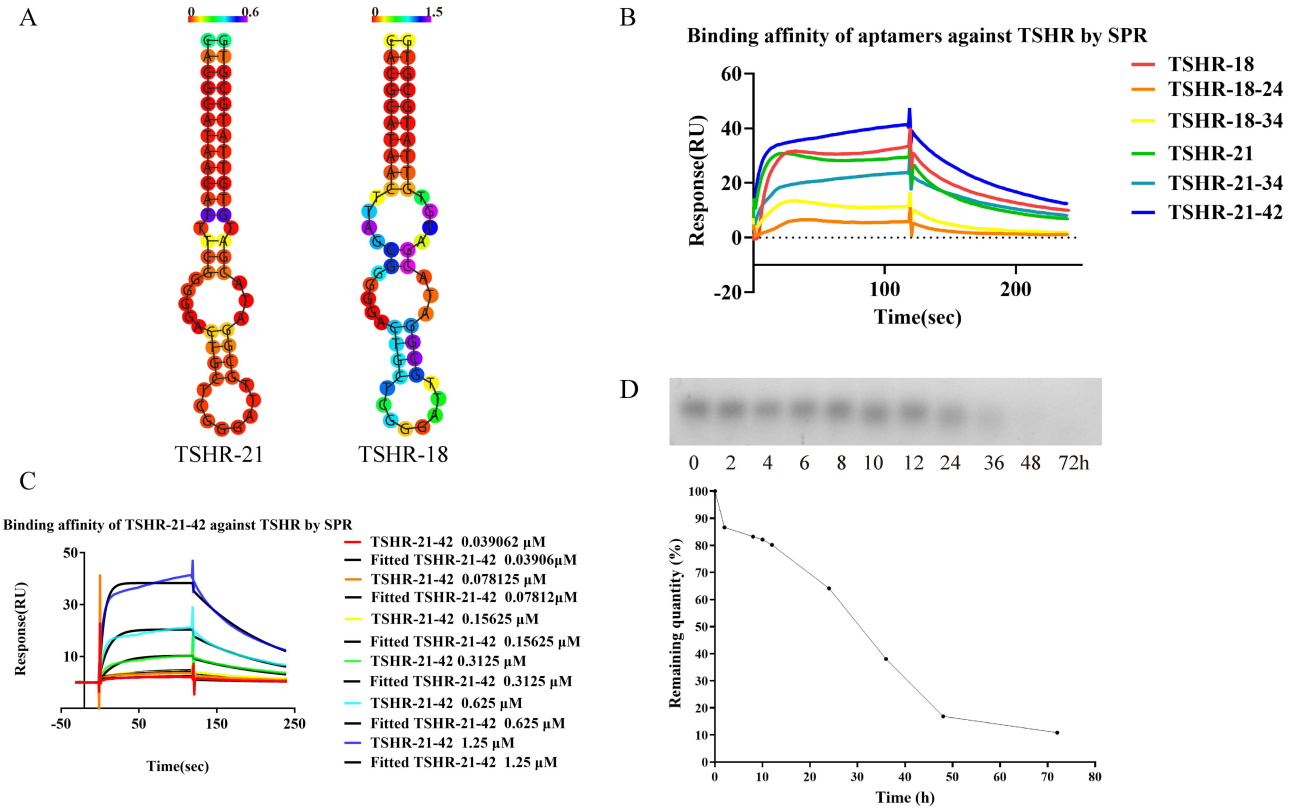

Figure 2 Optimization of the aptamer and determination of its stability in serum. (**A**) RNAFold determination of the secondary structure of the aptamers. (**B**) Truncation of the aptamers. (**C**) SPR determination of the equilibrium dissociation constant of the aptamer to TSHR. (**D**) Stability of the aptamer in serum.

the speed of degradation, however, subsequently decreased, with over 80% of TSHR-21-42 degraded after 48 h (Figure 2D).

TSHR-21-42 Binds to Fibrocytes

Although TSHR-21-42 was found to bind to TSHR, it was not clear whether this aptamer could bind to TSHR on cells. Fibrocytes were selected as model cells because of their pathogenic effect in TAO and their surface expression of TSHR. PBMCs from TAO patients were cultured, yielding adherent spindle cells (Figure 3A). Immunofluorescence staining showed that these cells expressed CD45, collagen I, and CD34, indicating that they were fibrocytes (Supplementary Figure 2). TSHR-21-42 was found to have a high affinity to these fibrocytes (Figure 3B and 3C), with an equilibrium dissociation constant of 61.96 nM (Supplementary Figure 3). Binding of TSHR-21-42 to fibrocytes was affected by an increase in temperature and a change in binding buffer. Incubation in serum at 37°C may facilitate the binding of TSHR-21-42 to fibrocytes (Figure 3D).

TSHR-21-42 Competes with Anti-TSHR Antibody for Binding and Internalization

To determine whether TSHR-21-42 competes with anti-TSHR antibody for binding sites on fibrocytes, molecular docking was simulated with HDOCK. The docking site of TSHR-21-42 on TSHR was similar to that of the anti-TSHR antibody M22 on TSHR, indicating a competitive relationship between TSHR-21-42 and M22 (Figure 4A). Coomassie brilliant blue staining of TSHR-21-42 binding proteins on fibrocytes showed that and the molecular weight of the bound protein was lower than 72 kd, consistent with its being TSHR (Supplementary Figure 4). Flow cytometry showed that the addition of anti-TSHR antibody to fibrocytes reduced the binding of TSHR-21-42, suggesting that TSHR-21-42 and anti-TSHR antibody have similar binding sites (Figure 4B). In addition, bound TSHR-21-42 was found

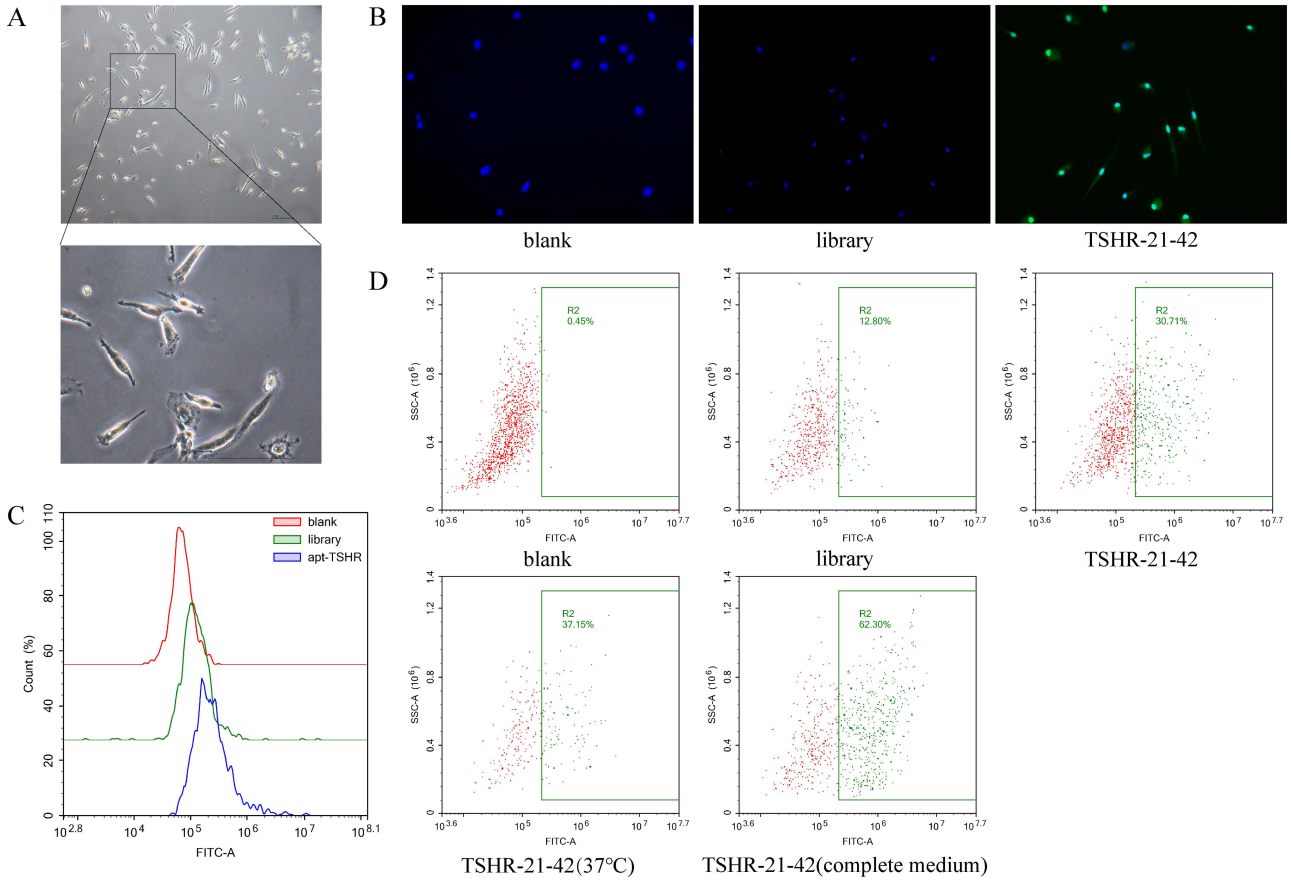

Figure 3 Affinity of the aptamer THSR-21-42 to fibrocytes. (**A**) Isolation of fibrocytes isolated from PBMCs. (**B** and **C**) Determination of the affinity of TSHR-21-42 to fibrocytes. (**D**) Assessment of aptamer affinity under different binding conditions.

to be internalized by fibrocytes, with only partial fluorescence lost after treating these cells with digestive enzymes (Figure 4C).

TSHR-21-42 in the Evaluation TAO

The clinical applications of TSHR-21-42 were evaluated by assessing this aptamer in 23 blood samples, four from healthy controls and 19 from patients with TAO; their basic clinical information is presented in Supplementary Table 2. TSHR-21-42 in TAO was initially evaluated by comparisons in healthy subjects and patients with TAO. Simple size analysis showed that more than two samples per group was sufficient to assess differences between groups. Flow cytometry analysis of samples from four healthy controls and five patients with TAO (Supplementary Figure 5) showed that the percentage of TSHR-positive fibrocytes, as determined by binding of TSHR-21-42, was significantly higher in TAO patients than in healthy controls, but that there was no difference between these two groups as determined by binding of the aptamer library (Figure 5A and 5B).

TSHR-positive fibrocytes in TAO patients, as determined using TSHR-21-42 and anti-TSHR antibody, were also compared. The ratio of fibrocytes to WBC correlated significantly using both measures (Supplementary Figure 6), as did the ratio of TSHR-positive fibrocytes to total fibrocytes (Figure 5C). To increase the practicality of TSHR-21-42 and provide an objective indicator for the stage of TAO, TSHR-21-42 was cultured with WBCs to detect TSHR-positive cells. The ratio of TSHR-positive cells to WBCs was higher for monocytes, granulocytes, and lymphocytes than other cells, with monocytes having the highest ratio (Supplementary Figure 7). Statistical analysis showed that the proportion of TSHR-positive monocytes differed significantly in patients with active and inactive TAO (Supplementary Figure 8), but was not associated with the severity of TAO, likely because of insufficient data (Supplementary Figure 9). Moreover,

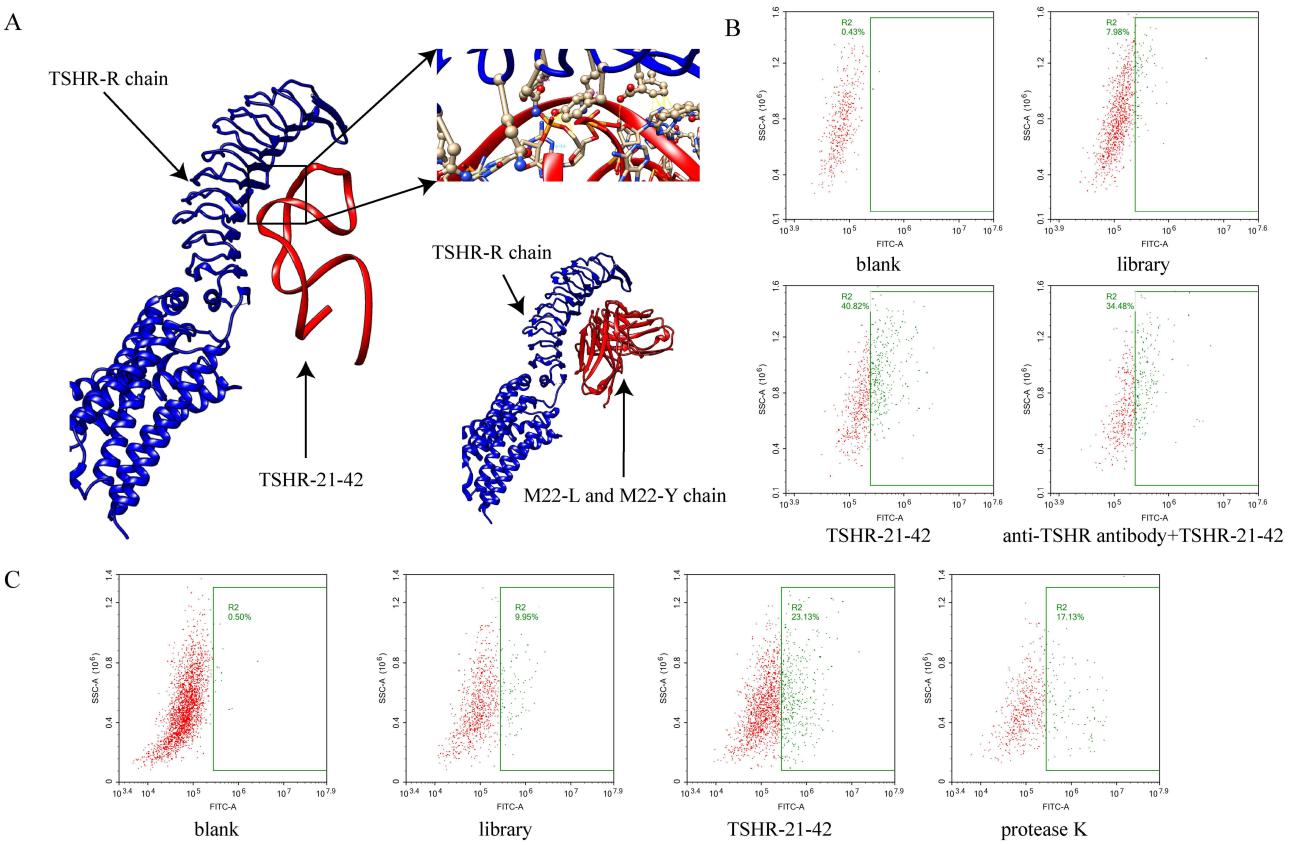

Figure 4 Mechanism underlying the binding of TSHR-21-42 to fibrocytes. (**A**) 3D molecular docking, showing that the binding sites of TSHR-21-42 and anti-TSHR antibody to fibrocytes were similar. (**B**) Competition of TSHR-21-42 with anti-TSHR antibody for binding to fibrocytes. (**C**) Internalization of TSHR-21-42 after binding to fibrocytes.

a positive linear relationship was observed between the proportion of TSHR-positive monocytes and CAS in patients with TAO (P<0.0001) (Figure 5D). Using a CAS cutoff of 3, linear regression analysis showed that TAO patients with >35.83% TSHR positive monocytes in PBMCs would have active stage disease.

Discussion

The present study describes an aptamer targeting TSHR, which was obtained through SELEX and optimized through truncation. This aptamer, TSHR-21-42, was found to bind to TSHR on fibrocytes with high affinity. Moreover, this aptamer may be clinically useful in distinguishing between TAO patients and healthy controls, as well as being an objective indicator of the clinical stage of TAO. Thus, TSHR-21-42 may be useful in the development of individualized treatment strategies for patients with TAO.

SELEX, the method used to obtain aptamers in the present study, was developed more than 30 years ago.[30] Many kinds of SELEX have been developed, based on both the target and process, including cell-SELEX, tissue-SELEX, and HT-SELEX.[31–33] All of these methods, however, maintain the basic logic of SELEX, including the continuous extraction of high-affinity aptamers and the discarding of low-affinity aptamers.[34] Altering the conditions of SELEX, such as temperature or binding buffer, would yield different types of aptamer.[35] In the present study, TSHR protein was the positive target, and SPR was used to evaluate binding capacity. The affinity of the aptamer was evaluated in isolated cells, as well as clinically. Evaluation of the affinity of the aptamer under different conditions showed satisfactory performance. These findings provided the basis for the clinical application of TSHR-21-42, to some extent.

TSHR is a 7-transmembrane domain G protein-coupled receptor expressed mainly in thyrocytes that is activated mainly upon binding TSH.[36] During the pathogenesis of TAO, TSHR not only promotes thyroid dysfunction but also participates in immune system dysfunction in the orbits through fibrocytes derived from bone marrow. IGF-1R may act as an important

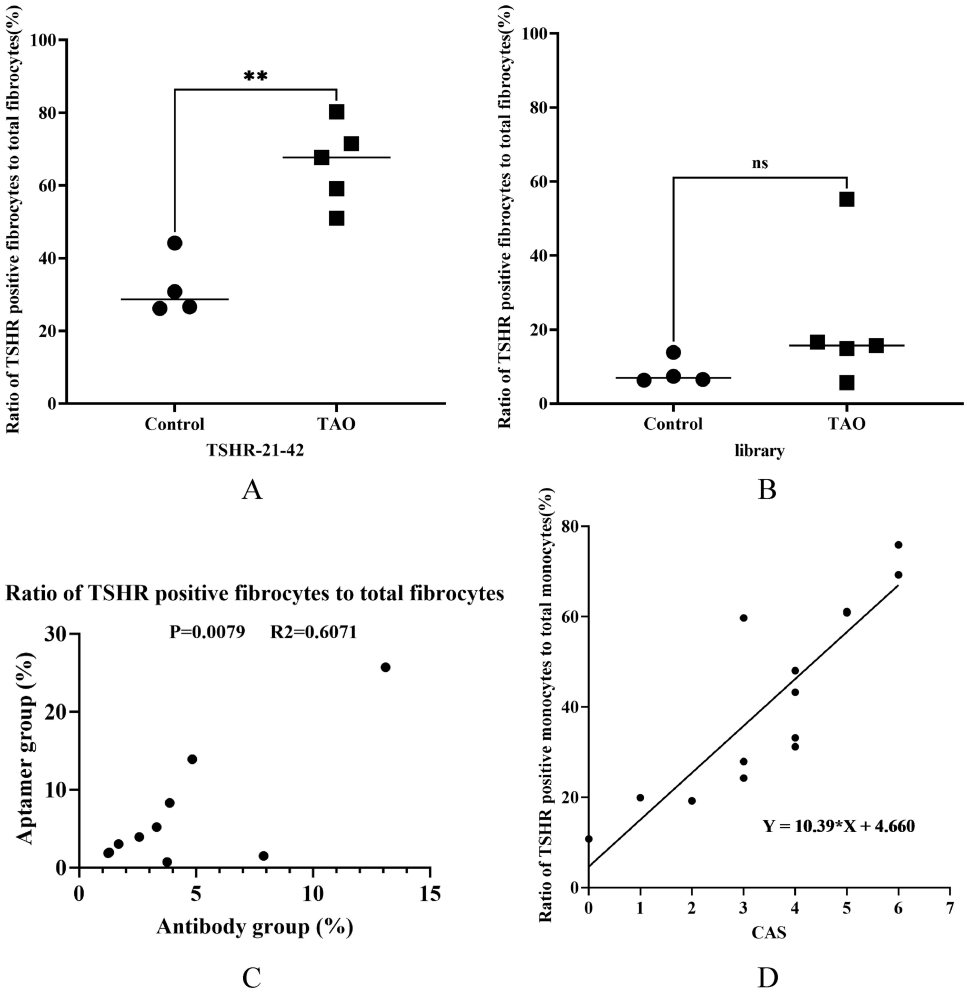

Figure 5 Clinical application of TSHR-21-42 in patients with TAO. (**A** and **B**) Binding of TSHR-21-42 and aptamer libraries to fibrocytes from patients with TAO and normal controls (**: P<0.01, ns: not significant). (**C**) Ratios of TSHR-positive fibrocytes to total fibrocytes, as determine with the aptamer TSHR-21-42 and anti-TSHR antibody. (**D**) Relationship between the percentage of TSHR positive monocytes and CAS in patients with TAO.

receptor during the pathogenesis of TAO, with teprotumumab, a monoclonal antibody directed against IGF1, being effective in the treatment of TAO.[37] However, the interactions between TSHR and IGF-1R are complex, with immunoglobulins binding directly to TSHR.[9,38] Based on its important role in TAO, this study selected TSHR as the positive target during SELEX. Aptamer detection of TSHR expression showed that this receptor correlated positively with disease activity of disease, with results consistent with those obtained using anti-TSHR antibody, but at much lower cost.[15,39]

Fibrocytes are a type of monocyte derived from bone marrow that function in immune reactions and repair of injury. These cells have been identified as circulating cells positive for CD45 and collagen I.[40,41] Moreover, fibrocytes have been shown to display an essential role in the pathogenesis of TAO, as well as express CD40 and participate in B cell immunity.[42] Fibrocytes were also found to differ from myofibroblasts and adipocytes.[43] Circulating fibrocytes also act as an accurate biomarker in uncomplicated appendicitis and pulmonary hypertension.[44,45] These results indicate that fibrocytes could be used to evaluate the stage of diseases, including TAO. In this study, fibrocytes were detected using TSHR targeting aptamers, with significant differences between TAO patients and healthy controls. Monocytes were also detected in the present study, with the percentages of monocytes correlating positively with CAS. This may facilitate the use of this aptamer as an indicator, as there was no need to distinguish fibrocytes from monocytes.

CAS is an important clinical indicator of the stage of TAO that has been used for disease classification and for designing individualized treatment. Because subjective staging by different physicians differed in individual patients.[46] efforts have been made to objectively evaluate disease activity. For example, fibulin-1 concentration has been used to

evaluate the activity of TAO, with concentrations over 625.33pg/mL indicating an active stage of disease.[47] MRI has also been used to evaluate activity, as MRI results differ during various stages of TAO.[48] TAO has also been accurately classified using machine learning methods.[49] All of these emerging technologies, however, are expensive, especially in their use of antibodies, and their findings do not correlate directly with treatment. In addition, current therapy, such as treatment with glucocorticoids, may affect the assessment of CAS, as glucocorticoids suppress inflammation and reduce the severity of disease.[13] The aptamer targeting TSHR is not only less expensive than antibody but may guide the treatment of TAO.

Coupling the aptamer targeting TSHR with fluorescein isothiocyanate isomer I (FITC) can enable aptamer bound to cells to be detected by flow cytometry. The possibility of non-specific binding suggests the need for caution in interpreting the results of quantitative analysis using the aptamer, especially when compared with the antibody targeting the same protein. Because of its high affinity, low cost and editability, this aptamer could be used to construct various types of biochemical or electrochemical sensors.[50]

TSHR has been associated with immune system dysfunction and in the pathogenesis of Graves' disease (GD) and TAO, suggesting that inhibiting TSHR activity may have a therapeutic effect in these conditions. Blocking TSHR using the antibody Ki-70 has been shown effective in the treatment of TAO and GD, suggesting that TSHR-21-42 may have similar activity in these diseases.[51,52] Aptamers targeting TSHR can be used in the development of drugs and testing methods. The high binding affinity of TSHR-21-42 to TSHR, as well as the ability to edit the aptamer, suggests that this aptamer could be used in the development of TSHR related drugs to treat diseases cure such as GD and TAO.

Although the present study found that the aptamer could bind TSHR with high affinity and compete with anti-TSHR antibody, the ability of the aptamer to bind TSHR in a more complex environment has not been determined. Although TSHR-21-42 could distinguish between TAO patients and healthy controls, showing a positive correlation between CAS and the percentage of monocytes, large-scale studies are needed to confirm these findings.

In conclusion, the present study described the development of an aptamer targeting TSHR. This aptamer, TSHR-21-42, bound to TSHR with high affinity, suggesting it could be used to evaluate the clinical stage of TAO.

Abbreviations

BSA, Bovine serum albumin; CAS, Clinical activity scores; EUGOGO, European Group on Graves' orbitopathy; GD, Graves' disease; HAS, Human serum albumin; PBMC, Peripheral blood mononuclear cells; SPR, Surface plasmon resonance; TAO, Thyroid-associated ophthalmopathy.

TSHR, Thyroid-stimulating hormone receptor; WBC, White blood cells.

Data Sharing Statement

The data that support the findings of this study are available from the corresponding author, WX, upon reasonable request.

Ethics Approval and Consent to Participate

The study was performed in accordance with the Declaration of Helsinki and was approved by the Institutional Review Board of The Third Xiangya Hospital of Central South University (NO: kuai 1 23004). Written informed consent was obtained from each subject.

Funding

This work was supported by the National Natural Science Foundation of China (82071006 and 82371104), the Fundamental Research Funds for the Central University of Central South University (2023ZZTS0327) and The Natural Science Foundation of Hunan Province (2023JJ30851).

Disclosure

The authors declare that they have no competing interests in this work.

References

1. Bahn RS. Graves' ophthalmopathy. *N Engl J Med*. 2010;362(8):726–738. doi:10.1056/NEJMra0905750
2. Smith TJ. Understanding pathogenesis intersects with effective treatment for thyroid eye disease. *J Clin Endocrinol Metab*. 2022;107(Suppl_1): S13–26. doi:10.1210/clinem/dgac328
3. Liu Z, Liu Y, Liu M, et al. PD-L1 inhibits t cell-induced cytokines and hyaluronan expression via the CD40-CD40L pathway in orbital fibroblasts from patients with thyroid associated ophthalmopathy. *Front Immunol*. 2022;13:849480. doi:10.3389/fimmu.2022.849480
4. Hei X, Lin B, Wu P, et al. Lutein targeting orbital fibroblasts attenuates fibrotic and inflammatory effects in thyroid-associated ophthalmopathy. *Exp Eye Res*. 2023;232:109515. doi:10.1016/j.exer.2023.109515
5. Chandra J, Samali A, Orrenius S. Triggering and modulation of apoptosis by oxidative stress. *Free Radic Biol Med*. 2000;29(3–4):323–333. doi:10.1016/S0891-5849(00)00302-6
6. Kim DW, Taneja K, Hoang T, et al. Transcriptomic profiling of control and thyroid-associated orbitopathy (TAO) orbital fat and TAO orbital fibroblasts undergoing adipogenesis. *Invest Ophthalmol Vis Sci*. 2021;62(9):24. doi:10.1167/iovs.62.9.24
7. Morshed SA, Ma R, Latif R, Davies TF. Mechanisms in graves eye disease: apoptosis as the end point of insulin-like growth factor 1 receptor inhibition. *Thyroid*. 2022;32(4):429–439. doi:10.1089/thy.2021.0176
8. Krieger CC, Neumann S, Marcus-Samuels B, Gershengorn MC. TSHR/IGF-1R cross-talk, Not IGF-1R stimulating antibodies, mediates graves' ophthalmopathy pathogenesis. *Thyroid*. 2017;27(5):746–747. doi:10.1089/thy.2017.0105
9. Krieger CC, Neumann S, Gershengorn MC. Is there evidence for IGF1R-stimulating abs in graves' orbitopathy pathogenesis? *Int J Mol Sci*. 2020;21(18):6561. doi:10.3390/ijms21186561
10. Diana T, Holthoff HP, Fassbender J, et al. A novel long-term graves' disease animal model confirmed by functional thyrotropin receptor antibodies. *Eur Thyroid J*. 2020;9(Suppl 1):51–58. doi:10.1159/000508790
11. Kahaly GJ, Diana T, Kanitz M, et al. Prospective trial of functional thyrotropin receptor antibodies in graves disease. *J Clin Endocrinol Metab*. 2020;105(4):e1006–14. doi:10.1210/clinem/dgz292
12. George A, Diana T, Langericht J, Kahaly GJ. Stimulatory thyrotropin receptor antibodies are a biomarker for graves' orbitopathy. *Front Endocrinol*. 2020;11:629925. doi:10.3389/fendo.2020.629925
13. Bartalena L, Kahaly GJ, Baldeschi L, et al. The 2021 European group on graves' orbitopathy (EUGOGO) clinical practice guidelines for the medical management of graves' orbitopathy. *Eur J Endocrinol*. 2021;185(4):G43–67. doi:10.1530/EJE-21-0479
14. Gillespie EF, Papageorgiou KI, Fernando R, et al. Increased expression of TSH receptor by fibrocytes in thyroid-associated ophthalmopathy leads to chemokine production. *J Clin Endocrinol Metab*. 2012;97(5):E740–6. doi:10.1210/jc.2011-2514
15. Basak M, Sanyal T, Kar A, et al. Peripheral blood mononuclear cells - Can they provide a clue to the pathogenesis of graves' orbitopathy? *Endocrine*. 2022;75(2):447–455. doi:10.1007/s12020-021-02865-0
16. Khoshbin Z, Shakour N, Iranshahi M, et al. Aptamer-based biosensors: promising sensing technology for diabetes diagnosis in biological fluids. *Curr Med Chem*. 2023;30(30):3441–3471.
17. Liu Y, Qian X, Ran C, et al. Aptamer-based targeted protein degradation. *ACS Nano*. 2023;17(7):6150–6164. doi:10.1021/acsnano.2c10379
18. Cao J, Zhang F, Xiong W. Discovery of aptamers and the acceleration of the development of targeting research in ophthalmology. *Int J Nanomed*. 2023;18:4421–4430. doi:10.2147/IJN.S418115
19. Alkhamis O, Canoura J, Ly PT, Xiao Y. Using exonucleases for aptamer characterization, engineering, and sensing. *Acc Chem Res*. 2023;56 (13):1731–1743. doi:10.1021/acs.accounts.3c00113
20. Li M, Yang G, Zheng Y, et al. NIR/pH-triggered aptamer-functionalized DNA origami nanovehicle for imaging-guided chemo-phototherapy. *J Nanobiotechnology*. 2023;21(1):186. doi:10.1186/s12951-023-01953-9
21. Zhang X, Zhang C, Li N, et al. Gold-bipyramid-based nanothernostics: FRET-mediated protein-specific sialylation visualization and oxygen-augmenting phototherapy against hypoxic tumor. *Anal Chem*. 2021;93(35):12103–12115. doi:10.1021/acs.analchem.1c02625
22. Darmostuk M, Rimpelova S, Gbelcova H, Ruml T. Current approaches in SELEX: an update to aptamer selection technology. *Biotechnol Adv*. 2015;33(6 Pt 2)):1141–1161. doi:10.1016/j.biotechadv.2015.02.008
23. Tian H, Wang Y, Li J, Li H. 中国甲状腺相关眼病诊断和治疗指南(2022年) [Chinese guideline on the diagnosis and treatment of thyroid-associated ophthalmopathy (2022)]. *Zhonghua Yan Ke Za Zhi*. 2022;58(9):646–668. Chinese. doi:10.3760/cma.j.cn112142-20220421-00201
24. Mourits MP, Prummel MF, Wiersinga WM, Koornneef L. Clinical activity score as a guide in the management of patients with Graves' ophthalmopathy. *Clin Endocrinol*. 1997;47(1):9–14. doi:10.1046/j.1365-2265.1997.2331047.x
25. Denman RB. Using RNAFOLD to predict the activity of small catalytic RNAs. *Biotechniques*. 1993;15(6):1090–1095.
26. Hanwell MD, Curtis DE, Lonie DC, et al. Avogadro: an advanced semantic chemical editor, visualization, and analysis platform. *J Cheminform*. 2012;4(1):17. doi:10.1186/1758-2946-4-17
27. Yan Y, Zhang D, Zhou P, et al. HDOCK: a web server for protein-protein and protein-DNA/RNA docking based on a hybrid strategy. *Nucleic Acids Res*. 2017;45(W1):W365–73. doi:10.1093/nar/gkx407
28. Peduzzi P, Concato J, Kemper E, et al. A simulation study of the number of events per variable in logistic regression analysis. *J Clin Epidemiol*. 1996;49(12):1373–1379. doi:10.1016/S0895-4356(96)00236-3
29. Austin PC, Steyerberg EW. The number of subjects per variable required in linear regression analyses. *J Clin Epidemiol*. 2015;68(6):627–636. doi:10.1016/j.jclinepi.2014.12.014
30. Tuerk C, MacDougal S, Gold L. RNA pseudoknots that inhibit human immunodeficiency virus type 1 reverse transcriptase. *Proc Natl Acad Sci U S A*. 1992;89(15):6988–6992. doi:10.1073/pnas.89.15.6988
31. Abreu R, Antunes D, Moreira A, et al. Next generation of ovarian cancer detection using aptamers. *Int J Mol Sci*. 2023;24(7):6315. doi:10.3390/ijms24076315
32. Li L, Wan J, Wen X, et al. Identification of a new DNA aptamer by tissue-SELEX for cancer recognition and imaging. *Anal Chem*. 2021;93 (19):7369–7377. doi:10.1021/acs.analchem.1c01445
33. Mukherjee S, Murata A, Ishida R, et al. HT-SELEX-based identification of binding pre-miRNA hairpin-motif for small molecules. *Mol Ther Nucleic Acids*. 2022;27:165–174. doi:10.1016/j.omtn.2021.11.021

34. Yang LF, Ling M, Kacherovsky N, Pun SH. Aptamers 101: aptamer discovery and in vitro applications in biosensors and separations. *Chem Sci*. 2023;14(19):4961–4978. doi:10.1039/D3SC00439B
35. Sola M, Menon AP, Moreno B, et al. Aptamers against live targets: is in vivo SELEX finally coming to the edge? *Mol Ther Nucleic Acids*. 2020;21:192–204. doi:10.1016/j.omtn.2020.05.025
36. Davies TF, Ando T, Lin RY, et al. Thyrotropin receptor-associated diseases: from adenomata to graves disease. *J Clin Invest*. 2005;115 (8):1972–1983. doi:10.1172/JCI26031
37. Douglas RS, Kahaly GJ, Patel A, et al. Teprotumumab for the treatment of active thyroid eye disease. *N Engl J Med*. 2020;382(4):341–352. doi:10.1056/NEJMoa1910434
38. Krieger CC, Neumann S, Gershengorn MC. TSH/IGF1 receptor crosstalk: mechanism and clinical implications. *Pharmacol Ther*. 2020;209:107502. doi:10.1016/j.pharmthera.2020.107502
39. Douglas RS, Afifiyan NF, Hwang CJ, et al. Increased generation of fibrocytes in thyroid-associated ophthalmopathy. *J Clin Endocrinol Metab*. 2010;95(1):430–438. doi:10.1210/jc.2009-1614
40. Bucala R, Spiegel LA, Chesney J, et al. Circulating fibrocytes define a new leukocyte subpopulation that mediates tissue repair. *Mol Med*. 1994;1 (1):71–81. doi:10.1007/BF03403533
41. Fernando R, Grisolia A, Lu Y, et al. Slit2 modulates the inflammatory phenotype of orbit-infiltrating fibrocytes in graves' disease. *J Immunol*. 2018;200(12):3942–3949. doi:10.4049/jimmunol.1800259
42. Mester T, Raychaudhuri N, Gillespie EF, et al. CD40 expression in fibrocytes is induced by TSH: potential synergistic immune activation. *PLoS One*. 2016;11(9):e162994. doi:10.1371/journal.pone.0162994
43. Antonelli A, Ferrari SM, Fallahi P. Slit2 regulation of hyaluronan and cytokine synthesis in fibrocytes in thyroid-associated ophthalmopathy. *J Clin Endocrinol Metab*. 2021;106(4):e1907–8. doi:10.1210/clinem/dgaa959
44. Liu X, Li X, Duan J, et al. The percentage of circulating fibrocytes is associated with increased morbidity of pulmonary hypertension in patients on hemodialysis. *Semin Dial*. 2023;37(1):43–51.
45. Zarog M, O'Leary P, Kiernan M, et al. Circulating fibrocyte percentage and neutrophil-lymphocyte ratio are accurate biomarkers of uncomplicated and complicated appendicitis: a prospective cohort study. *Int J Surg*. 2023;109(3):343–351. doi:10.1097/JS9.0000000000000234
46. Nie T, Lamb YN. Teprotumumab: a review in thyroid eye disease. *Drugs*. 2022;82(17):1663–1670. doi:10.1007/s40265-022-01804-1
47. Hu H, Liang L, Zheng X, et al. Fibulin-1: a novel biomarker for predicting disease activity of the thyroid-associated ophthalmopathy. *Eye*. 2022;37 (11):2216–2219. doi:10.1038/s41433-022-02318-6
48. Jiang M, Song X, Zhang H, et al. The combination of T2-mapping value of lacrimal gland and clinical indicators can improve the stage prediction of Graves' ophthalmopathy compared to clinical activity scores. *Endocrine*. 2022;78(2):321–328. doi:10.1007/s12020-022-03167-9
49. Moon JH, Shin K, Lee GM, et al. Machine learning-assisted system using digital facial images to predict the clinical activity score in thyroid-associated orbitopathy. *Sci Rep*. 2022;12(1):22085. doi:10.1038/s41598-022-25887-8
50. Wu T, Yagati AK, Min J. Electrochemical detection of different foodborne bacteria for point-of-care applications. *Biosensors*. 2023;13(6):641. doi:10.3390/bios13060641
51. Duan J, Xu P, Luan X, et al. Hormone- and antibody-mediated activation of the thyrotropin receptor. *Nature*. 2022;609(7928):854–859. doi:10.1038/s41586-022-05173-3
52. Ryder M, Wentworth M, Algeciras-Schimnich A, et al. Blocking the thyrotropin receptor with K1-70 in a patient with follicular *thyroid* cancer, graves' disease, and graves' ophthalmopathy. *Thyroid*. 2021;31(10):1597–1602. doi:10.1089/thy.2021.0053